Mol Cell Biochem (2014) 389:119–132
DOI 10.1007/s11010-013-1933-y

# Hepatic bile acid metabolism and expression of cytochrome P450 and related enzymes are altered in *Bsep*$^{-/-}$ mice

**Eugene Hrycay · Dana Forrest · Lin Liu · Renxue Wang · Jenny Tai · Anand Deo · Victor Ling · Stelvio Bandiera**

Received: 10 July 2013 / Accepted: 18 December 2013 / Published online: 8 January 2014


**Abstract** The bile salt export pump (BSEP/Bsep; gene symbol *ABCB11*/*Abcb11*) translocates bile salts across the hepatocyte canalicular membrane into bile in humans and mice. In humans, mutations in the *ABCB11* gene cause a severe childhood liver disease known as progressive familial intrahepatic cholestasis type 2. Targeted inactivation of mouse Bsep produces milder persistent cholestasis due to detoxification of bile acids through hydroxylation and alternative transport pathways. The purpose of the present study was to determine whether functional expression of hepatic cytochrome P450 (CYP) and microsomal epoxide hydrolase (mEH) is altered by Bsep inactivation in mice and whether bile acids regulate CYP and mEH expression in *Bsep*$^{-/-}$ mice. CYP expression was determined by measuring protein levels of Cyp2b, Cyp2c and Cyp3a enzymes and CYP-mediated activities including lithocholic acid hydroxylation, testosterone hydroxylation and alkoxyresorufin *O*-dealkylation in hepatic microsomes prepared from female and male *Bsep*$^{-/-}$ mice fed a normal or cholic acid (CA)-enriched diet. The results indicated that hepatic lithocholic acid hydroxylation was catalyzed by Cyp3a/Cyp3a11 enzymes in *Bsep*$^{-/-}$ mice and that 3-ketocholanoic acid and murideoxycholic acid were major metabolites. CA feeding of *Bsep*$^{-/-}$ mice increased hepatic Cyp3a11 protein levels and Cyp3a11-mediated testosterone 2β-, 6β-, and 15β-hydroxylation activities, increased Cyp2b10 protein levels and Cyp2b10-mediated benzyloxyresorufin *O*-debenzylation activity, and elevated Cyp2c29 and mEH protein levels. We propose that bile acids upregulate expression of hepatic Cyp3a11, Cyp2b10, Cyp2c29 and mEH in *Bsep*$^{-/-}$ mice and that Cyp3a11 and multidrug resistance-1 P-glycoproteins (Mdr1a/1b) are vital components of two distinct pathways utilized by mouse hepatocytes to expel bile acids.

**Keywords** Bile acid metabolism · *Bsep*$^{-/-}$ mice · Cholestasis · Cyp3a11 · Cyp2b10 · Microsomal epoxide hydrolase

E. Hrycay · J. Tai · A. Deo · S. Bandiera (✉)
Faculty of Pharmaceutical Sciences, The University of British Columbia, Vancouver, BC V6T1Z3, Canada
e-mail: bandiera@mail.ubc.ca

D. Forrest · L. Liu · R. Wang · V. Ling
British Columbia Cancer Research Center, Vancouver, BC V5Z1L3, Canada

## Introduction

Mammalian cytochrome P450 (CYP) enzymes play a central role in the biotransformation of lipid-soluble xenobiotics such as drugs, carcinogens and environmental chemical pollutants, and endogenous compounds such as cholesterol, bile acids and steroid hormones [1–3]. Bile acids are amphipathic detergent-like molecules that are biosynthesized from cholesterol in the liver and are secreted, after conjugation with glycine or taurine, into bile ducts and then into the gallbladder or duodenum [4–9]. Biliary secretion of bile acids plays a vital role in the solubilization and absorption of lipid-soluble nutrients and vitamins, maintenance of cholesterol homeostasis and promotion of bile flow [4–9]. In addition, bile acids serve as hepatic signaling molecules through activation of nuclear receptors such as the farnesoid X receptor (FXR/Fxr), which functions in the transcriptional regulation of genes involved in bile acid synthesis and transport [9–12]. Impairment of normal bile flow into the duodenum causes a pathophysiological condition known as cholestasis, which is characterized by the accumulation of bile acids in the

liver and subsequent liver cell injury due to the inherent cytotoxicity of bile acids [5, 8].

The bile salt export pump (BSEP/Bsep; gene symbol *ABCB11*/*Abcb11*), originally known as sister of P-glycoprotein (SPGP/Spgp) [8], is the major hepatic ATP-binding cassette (ABC) bile salt transporter in humans and mice [8]. BSEP/Bsep functions by translocating bile salts across the hepatocyte canalicular membrane into the bile canaliculus [8]. It is closely related to the multidrug resistance-1 P-glycoprotein (MDR1/Mdr1; gene symbol *ABCB1*/*Abcb1*), which mediates the efflux of steroids, drugs and other xenobiotics from hepatocytes and other cells [8, 9, 13–15]. *BSEP*/*Bsep* mRNA expression is increased when hepatic bile acid levels are elevated due to direct activation of the *ABCB11*/*Abcb11* gene by bile acids acting through FXR/Fxr [9–12]. Induction of BSEP/Bsep leads, in turn, to enhanced efflux of bile salts from the hepatocyte and returns intrahepatocellular bile acid levels to normal [9]. Thus, FXR/Fxr functions as a hepatic intracellular bile acid sensor and a major regulator of bile acid homeostasis [9, 10].

In humans, genetic defects of the *ABCB11* gene result in a severe childhood liver disease known as progressive familial intrahepatic cholestasis type 2 (PFIC2) [16]. PFIC2 is characterized by greatly reduced bile flow, extensive accumulation of bile salts in the liver, growth retardation, jaundice, hepatomegaly, cholangiopathy, elevated aminotranferase and alkaline phosphatase activity, cirrhosis and hepatocellular carcinoma, leading to hepatic failure and death in childhood unless a partial external biliary diversion, ileal exclusion, or liver transplantation is performed [8, 12, 15–18]. Targeted inactivation of mouse Bsep produces a milder but persistent form of intrahepatic cholestasis characterized by a marked elevation in hepatic bile salt levels and only a slight reduction in bile flow [8]. *Bsep*$^{-/-}$ mice also produce novel tetrahydroxylated bile acids that are less toxic and more hydrophilic than the bile acids normally found in wild-type mice [8, 19, 20]. Wang et al. [8, 15] proposed that the more benign cholestatic phenotype displayed by *Bsep*$^{-/-}$ mice was the result of their ability to detoxify bile salts by two compensatory mechanisms involving increased bile acid hydroxylation and upregulation of an alternative canalicular bile salt transport system that utilizes Mdr1a/1b transporters to efflux excess bile acids from the hepatocyte.

Hepatic microsomal epoxide hydrolase (EC 3.3.2.3; mEH; gene symbol *EPHX1*) is a bifunctional protein that can hydrolyze chemical epoxide intermediates of xenobiotic [21–23] and endogenous compounds [24] formed by the oxidative action of CYP enzymes. In addition, mEH anchored in the sinusoidal plasma membrane of hepatocytes can mediate the $Na^+$-dependent uptake of bile salts from portal blood into hepatocytes of humans and rodents [24–30], while an isoform of mEH localized in the smooth endoplasmic reticular membrane of rats can transport bile salts into the lumen of endoplasmic reticulum vesicles, which can then expel the bile salts from the hepatocyte into bile by vesicular transport [31–35]. It would be interesting to determine whether mouse hepatic mEH protein levels are upregulated in response to Bsep inactivation and increased hepatic bile acid levels.

Because hydrophobic bile acids are inherently cytotoxic, their formation and elimination must be tightly regulated. CYP-mediated biotransformation is an effective mechanism for reducing the toxicity of bile acids in the hepatocyte and is considered a first line of defense against bile acid-elicited hepatotoxicity. Human and rat CYP3A enzymes can metabolize and detoxify a variety of bile acids including lithocholic acid (3α-hydroxy-5β-cholan-24-oic acid) [36–40], deoxycholic acid (3α,12α-dihydroxy-5β-cholan-24-oic acid) [37], chenodeoxycholic acid (3α,7α-dihydroxy-5β-cholan-24-oic acid) [36, 37, 41] and cholic acid (CA) (3α,7α,12α-trihydroxy-5β-cholan-24-oic acid) [37, 41]. The involvement of mouse hepatic CYP enzymes in the biotransformation and detoxification of bile acids has been suggested but not conclusively established.

CA is a major hepatic bile acid in humans and mice and is often added to the diet of mice to elicit cholestasis. Wang et al. [17] fed female and male *Bsep*$^{-/-}$ mice, which display a mild form of cholestasis, a CA-enriched diet to elicit a more severe cholestasis characterized by weight loss, jaundice and elevated plasma and hepatic bile acid levels in female/male mice, liver cell damage and cholangiopathy in female mice, and loss of hepatic cell organelles, marked hepatocellular necrosis/apoptosis and high mortality rates in male mice [17]. In addition, mRNA expression of hepatic canalicular membrane transporters (Mdr1a/1b), sinusoidal membrane multidrug resistance protein bile acid efflux transporters (Mrp3, Mrp4), nuclear receptors (pregnane X receptor, Pxr) and CYP enzymes (Cyp2b10, Cyp3a11, Cyp3a16) was upregulated in CA-fed *Bsep*$^{-/-}$ mice [17]. Thus, *Bsep*$^{-/-}$ mice fed a CA-enriched diet can serve as a model for exploring the biochemical consequences and molecular pathways associated with cholestasis.

To develop a better understanding of bile acid metabolism and detoxification, along with the role of bile acids in regulating hepatic CYP and mEH expression in mice, we measured protein levels of Cyp2b, Cyp2c, Cyp3a, other CYP enzymes and mEH, and CYP-mediated lithocholic acid hydroxylation, testosterone hydroxylation and alkoxyresorufin *O*-dealkylation activities in hepatic microsomes prepared from female and male *Bsep*$^{-/-}$ mice fed a normal diet or a CA-enriched diet. Our objectives were to ascertain (1) if hepatic CYP and mEH protein expression and CYP-mediated enzyme activities are altered as a

consequence of Bsep inactivation, (2) if dietary CA administration alters hepatic CYP and mEH protein expression and CYP-mediated enzyme activities in *Bsep*$^{-/-}$ mice, and (3) if bile acids regulate hepatic CYP and mEH protein expression in *Bsep*$^{-/-}$ mice. The study was also designed to identify the hepatic CYP enzymes involved in lithocholic acid metabolism in *Bsep*$^{-/-}$ mice.

## Materials and methods

### Chemicals and reagents

CA was obtained from ICN Biochemicals (Cleveland, OH). Lithocholic acid, hyodeoxycholic acid (3α,6α-dihydroxy-5β-cholan-24-oic acid), isolithocholic acid (3β-hydroxy-5β-cholan-24-oic acid), 3-ketocholanoic acid (3-oxo-5β-cholan-24-oic acid), β-muricholic acid (3α,6β,7β-trihydroxy-5β-cholan-24-oic acid), and murideoxycholic acid (3α,6β-dihydroxy-5β-cholan-24-oic acid) were purchased from Steraloids Inc. (Newport, RI). Deuterated cholic-2,2,4,4-$d_4$ acid was a generous gift from Dr. Jan Palaty (Children's and Women's Health Center, Vancouver, BC, Canada). Dexamethasone (DEX), β-naphthoflavone (NF), and sodium phenobarbital (PB) were obtained from Sigma-Aldrich (St. Louis, MO). Alkaline phosphatase-labeled rabbit anti-sheep immunoglobulin G (IgG) was purchased from Kirkegaard & Perry Laboratories (Gaithersburg, MD), donkey anti-sheep IgG was obtained from Sigma-Aldrich and goat anti-rabbit F[ab′]$_2$ IgG was acquired from BioSource International (Camarillo, CA). Other reagents were purchased from sources cited earlier [17, 42].

### Animal treatment and preparation of hepatic microsomes

Wild-type mice and mutant homozygous *Bsep*$^{-/-}$ mice were generated by crossing female heterozygous *Bsep*$^{+/-}$ mice on a FVB/NJ genetic background and male *Bsep*$^{+/-}$ mice on a C57BL/6J genetic background [8]. Wild-type and *Bsep*$^{-/-}$ mice on a FVB/NJ genetic background are better breeders than C57BL/6J mice, but both strains are similar in their responses to Bsep inactivation [17]. Mice were cared for in accordance with the principles and guidelines of the Canadian Council on Animal Care under an approved protocol of The University of British Columbia.

Adult female and male wild-type and *Bsep*$^{-/-}$ (FVB/NJ × C57BL/6J) mice were fed (ad libitum) a normal diet (Pico Lab Rodent Diet 20, PMI LabDiet, Richmond, IN) or a CA-enriched diet (Pico Lab Rodent Diet 20 supplemented with 0.5 % CA) for 4 days. Mice were then killed, livers were quickly excised from each mouse and hepatic microsomes were prepared, as described previously [43], from pooled liver homogenates of each group (4–7 mice per group). Individual hepatic microsomes were also prepared from individual livers isolated from adult female and male wild-type and *Bsep*$^{-/-}$ (FVB/NJ) mice fed a normal diet (ad libitum) (4 or 6 mice per group). In addition, adult female wild-type C57BL/6 mice were treated with the following xenobiotics (NF, Cyp1a1/1a2 inducer; PB, Cyp2b10 and Cyp2c29 inducer; DEX, Cyp3a11 inducer) to induce hepatic Cyp expression as described previously [43]. The mice were treated, via intraperitoneal injection, with corn oil (10 ml/kg/day, $n = 27$), NF in corn oil (27 mg/kg/day, $n = 27$), PB in saline (102 mg/kg/day, $n = 25$) or DEX in corn oil (50 mg/kg/day, $n = 25$) for 3 consecutive days and were killed 24 h after the last injection. Hepatic microsomes were prepared from pooled livers. All hepatic microsome preparations were stored as aliquots at −80 °C until required.

### Total CYP and protein concentrations and enzyme assays

Total CYP [44] and protein [45] concentrations were measured according to the cited procedures. Testosterone hydroxylation activities were determined using a high performance liquid chromatography assay [46]. Benzyloxyresorufin *O*-debenzylase (BROD), ethoxyresorufin *O*-deethylase (EROD) and methoxyresorufin *O*-demethylase (MROD) activities were measured by the fluorometric assay of Burke et al. [47].

### Lithocholic acid hydroxylation assay

The lithocholic acid hydroxylation assay was performed as described previously [38]. Assay conditions were optimized for mouse hepatic microsomal protein and substrate concentrations and for time of incubation. Briefly, assays were performed in duplicate and mixtures containing 46.5 mM potassium phosphate buffer (pH 7.4), hepatic microsomal protein (0.5 mg/ml), lithocholic acid (100 or 250 μM) and 1 mM NADPH were incubated at 37 °C for 30 min in a final volume of 1 ml. Reactions were terminated with 4 ml of dichloromethane/isopropanol (80:20) and metabolites were extracted and reconstituted in 0.2 ml of mobile phase. Metabolites were resolved, detected and identified by a liquid chromatography/mass spectrometry (LC/MS)-based assay. Chemical structures of the bile acids, as well as a representative chromatogram illustrating their resolution, are shown in a previous report [38]. Metabolites were identified by comparing their retention times and mass to charge ratios (*m/z*) with those of authentic standards. The internal standard, cholic-2,2,4,4-$d_4$ acid (molecular mass 412.57), was monitored at *m/z* 411. β-Muricholic acid (molecular mass 408.57) was monitored at *m/z* 407.

Hyodeoxycholic acid and murideoxycholic acid (molecular mass 392.57) were monitored at *m*/*z* 391. Isolithocholic acid and lithocholic acid (molecular mass 376.57) were monitored at *m*/*z* 375. 3-Ketocholanoic acid (molecular mass 374.56) was monitored at *m*/*z* 373. Metabolites were quantified using calibration plots of the peak area ratio of authentic standard and internal standard plotted against concentration of authentic standard.

### Recombinant and purified enzymes and antibodies

Sf9 insect cell microsomes containing mouse recombinant Cyp2a4 (rCyp2a4) and rCyp2a5 proteins were kindly provided by Drs. S. Murphy and L. von Weymarn (University of Minnesota). Purified rat CYP1A1, CYP1A2, CYP2B1, CYP2C11, mEH and rat rCYP3A1 were used as calibration standards in immunoblot assays because purified mouse CYP and mEH proteins were not available. Rat CYP1A1, CYP2B1, CYP2C11 and mEH were purified as described previously [43, 46, 48, 49]. Purified rat CYP1A2 and CYP2A1 were kindly provided by W. Levin (Hoffmann-La Roche Inc.) and Dr. A. Parkinson (University of Kansas Medical Center), respectively. Rat rCYP3A1 was purchased from BD Gentest Corp. (Woburn, MA). A NADPH-cytochrome P450 oxidoreductase (reductase) internal standard was not available.

Rabbit anti-mouse polyclonal Cyp2c29 IgG was kindly donated by Dr. R. Meyer and M. Ditter (University of Freiburg, Germany). This antibody recognizes a major protein, identified as Cyp2c29, in mouse hepatic microsomes as described previously [50]. In other experiments, polyclonal antibodies against rat mEH, reductase and CYP enzymes were used to probe immunoblots containing mouse hepatic proteins. Anti-rat mEH IgG was raised in rabbits immunized with homogeneous mEH protein as described previously [46, 49]. Rabbit anti-rat reductase and anti-rat CYP4A IgG were obtained from Chemicon International Inc. (Mississauga, Ontario, Canada). Rabbit polyspecific anti-rat CYP1A2, anti-CYP2B1, anti-CYP2C11 and anti-CYP3A1 IgG were prepared as described previously [42, 46, 48]. Sheep anti-rat CYP2A1 IgG was provided by Dr. P. Thomas (Rutgers—The State University of New Jersey). Anti-CYP1A2 IgG reacts with rat CYP1A1 and CYP1A2 [48] and recognizes Cyp1a2 in mouse hepatic microsomes, while recognizing Cyp1a1 only in microsomes of NF-treated mice [43]. Anti-CYP2A1 IgG reacts with rat CYP2A1 and CYP2A2 [46] and with mouse rCyp2a4 and rCyp2a5, and recognizes the major Cyp2a5 and minor Cyp2a4 mouse microsomal proteins. Anti-CYP2B1 IgG reacts with rat CYP2B1, CYP2B2 and a third CYP2B protein [42] and with two major proteins, Cyp2b9 and Cyp2b10, in mouse microsomes. Anti-CYP2C11 IgG reacts with rat CYP2C6, CYP2C11 and other CYP2C proteins [46] and recognizes one major mouse Cyp2c protein identified as Cyp2c29 and another unidentified Cyp2c protein. Anti-CYP3A1 IgG cross-reacts with rat CYP3A1, CYP3A2 and CYP3A18 [48] and recognizes two major Cyp3a proteins, Cyp3a11 and Cyp3a41, in mouse microsomes. Anti-CYP4A IgG reacts with rat CYP4A1, CYP4A2 and CYP4A3 and recognizes one major unidentified mouse Cyp4a protein.

### Immunoblot analysis

Hepatic mouse CYP and mEH enzymes were identified and protein levels were measured by immunoblot analysis. Liver microsomal proteins were separated by discontinuous SDS-PAGE, transferred onto nitrocellulose and probed with antibodies against Cyp1a, Cyp2a, Cyp2b, Cyp2c, Cyp3a, Cyp4a, mEH and reductase proteins as previously described [42, 48]. Microsomal protein, at the concentrations indicated below, was applied to the gels in a volume of 20 μl/lane: 5 μg for Cyp1a, 5 or 10 μg for Cyp2a, 10 μg for Cyp2b, 1 μg for Cyp2c, 2.5 or 5 μg for Cyp3a, 40 or 60 μg for Cyp4a, 5 μg for mEH and 10 μg for reductase measurement. An appropriate concentration of calibration standard, in a 20 μl volume/lane, consisting of mouse rCyp2a4 and rCyp2a5 (0.2–0.5 pmol) or rat CYP2A1 (0.25 pmol), CYP1A1 (0.1 pmol), CYP1A2 (0.1 pmol), CYP2B1 (0.125 pmol), CYP2C11 (0.125 pmol), rCYP3A1 (0.125 pmol) and mEH (0.025 μg) was also applied. Proteins were resolved by electrophoresis for 3.5 h except Cyp3a proteins that required 5 h for optimal resolution. Nitrocellulose membranes were incubated with the following anti-rat primary antibodies: anti-CYP1A (1:1,000 dilution), anti-CYP2A (10 μg/ml), anti-CYP2B (2 μg/ml), anti-CYP2C (15 μg/ml), anti-CYP3A (15 μg/ml), anti-CYP4A (1:1,000 dilution), anti-mEH (10 μg/ml) and anti-reductase (1:10,000 dilution) IgG. Bound primary antibody was located by incubating immunoblots with secondary antibody (alkaline phosphatase-conjugated rabbit anti-sheep, donkey anti-sheep and goat anti-rabbit IgG) at a 1:500, 1:1,000 and 1:3,000 dilution, respectively. Immunoreactive protein bands were detected with substrate solution and were quantified by densitometric analysis. Quantities of microsomal protein and standard were chosen that gave a linear response upon reaction with antibody and development with substrate solution. The amount of immunoreactive protein was calculated in terms of relative optical density units per mg of microsomal protein using purified or recombinant rat standards.

### RT-PCR analysis

For real-time RT-PCR analysis, RNA was extracted from frozen livers of 4 FVB/NJ mice per group using Absolutely RNA RT-PCR Miniprep kit from Stratagene (La Jolla, CA). Reverse transcriptions were performed with

Superscript First-Strand Synthesis System for RT-PCR from Invitrogen (San Diego, CA). RT-PCR reactions were conducted in a PRISM 7900HT Sequence Detection System from Applied Biosystems (Foster City, CA) [17].

### Data analysis

For experiments involving microsomes prepared from individual livers of FVB/NJ mice, data are presented as the mean ± SE for each group. Differences between mean values were assessed by the nonparametric Mann–Whitney test. Correlation analysis involving enzyme activities and CYP protein levels was performed using GraphPad InStat version 3.0 software (GraphPad Software, San Diego, CA). Differences with a $P$ value of $<0.05$ were considered to be statistically significant.

## Results

### Effect of Bsep inactivation on hepatic CYP and mEH expression

Antibodies raised against rat CYP2B1, CYP3A1 and other proteins have been routinely used to probe immunoblots containing orthologous mouse Cyp2b10, Cyp3a11 and other proteins, respectively [51–54]. In the present study, mouse hepatic CYP proteins were identified on the basis of their relative electrophoretic mobility on polyacrylamide gels, reactivity with CYP antibodies, sex-dependent expression and pattern of induction, as described in Figs. 1 and 2 and Table 1. Relative protein levels of Cyp2a, Cyp2b, Cyp3a, other CYP enzymes and mEH were quantified in microsomes prepared from individual livers of *Bsep*$^{-/-}$ and wild-type FVB/NJ mice. The results (see Table 1) indicate that hepatic microsomal Cyp3a11 protein levels were significantly greater (2.1- and 2.5-times) in male and female *Bsep*$^{-/-}$ mice, respectively, compared to wild-type mice. In contrast, Cyp3a41 protein levels were significantly lower (1.7-times) in female *Bsep*$^{-/-}$ mice. Hepatic levels of the unidentified Cyp4a protein were significantly greater (5-times) in male, and significantly lower (2-times) in female, *Bsep*$^{-/-}$ mice, indicating a sex-dependent regulation. Hepatic mEH protein levels were 2.8- and 1.5-times greater in female and male *Bsep*$^{-/-}$ mice, respectively. We also quantified relative mRNA levels of several *Cyp3a* genes in individual livers of female and male *Bsep*$^{-/-}$ and wild-type FVB/NJ mice. The results indicate that *Cyp3a11* and *Cyp3a16* mRNA levels were significantly greater (2.0- to 2.6-times) in male and female *Bsep*$^{-/-}$ mice compared to wild-type mice (Table 2).

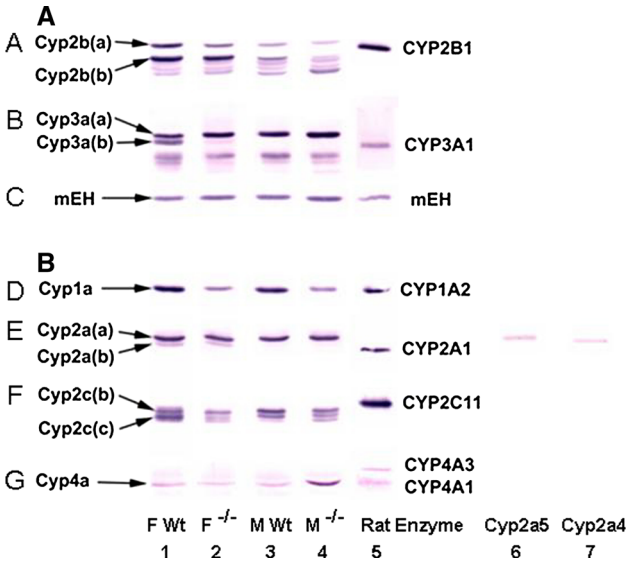


**Fig. 1** Immunoblots of microsomal CYP proteins isolated from pooled livers of *Bsep*$^{-/-}$ and wild-type (FVB/NJ × C57BL/6J) mice fed the normal diet. Immunoblots were probed with polyclonal antibodies prepared against rat CYP and mEH proteins. Representative immunoblots for Cyp2b, Cyp3a and mEH are illustrated in **a** and immunoblots for Cyp1a, Cyp2a, Cyp2c and Cyp4a are shown in **b**. *Lanes 1–4* contained hepatic microsomes from female wild-type (F Wt) (*lane 1*), F *Bsep*$^{-/-}$ (F$^{-/-}$) (*lane 2*), male Wt (M Wt) (*lane 3*), and M *Bsep*$^{-/-}$ (M$^{-/-}$) (*lane 4*) mice. (**a**), *lane 5* in *panels A, B, and C* contained rat CYP2B1 (0.125 pmol), rCYP3A1 (0.125 pmol), and mEH (0.025 μg), respectively. Anti-CYP2B IgG detected a major band, Cyp2b(a) (*panel A, upper band, lanes 1–4*), identified as Cyp2b10, and a female-predominant band, Cyp2b(b) (*lanes 1 and 2*), identified as Cyp2b9 that migrated just below Cyp2b(a). Anti-CYP3A IgG detected a major band, Cyp3a(a) (*panel B, upper band, lanes 1–4*), identified as Cyp3a11 and a female-predominant band, Cyp3a(b) (*lanes 1 and 2*), identified as Cyp3a41 that migrated just below Cyp3a(a). **b** *lane 5* in *panels D, E, F, and G* contained rat CYP1A2 (0.1 pmol), CYP2A1 (0.25 pmol), CYP2C11 (0.125 pmol) and hepatic microsomes (40 μg protein) from clofibrate-pretreated male rats (see Table 1), respectively. Anti-CYP1A IgG detected one major band (*panel D*) that corresponds to Cyp1a2. Anti-CYP2A IgG detected one major band, Cyp2a(a) (*panel E*, *upper band*, *lanes 1*–4), and a minor female-predominant band, Cyp2a(b) (*lower band*, *lanes 1 and* 2). Cyp2a(a) exhibited a similar electrophoretic mobility to rCyp2a5 (0.5 pmol, *lane 6*) that had a smaller mobility than rCyp2a4 (0.5 pmol, *lane 7*). Anti-CYP2C IgG detected a strong band, Cyp2c(b) (*panel F, upper band, lanes 1–4*), identified as Cyp2c29 and another unidentified band, Cyp2c(c), which migrated just below Cyp2c(b). Anti-CYP4A IgG detected one major unidentified Cyp4a band (*panel G*, *lanes 1–4*). Because a rat CYP4A standard was not available, liver microsomes isolated from male rats that had been pretreated with clofibrate (400 mg/kg/day × 4 days) to induce CYP4A proteins was used as a reference (*panel G*, *lane 5*, contained 60 μg of microsomal protein from clofibrate-pretreated rats). The two protein bands detected in *lane 5* were identified, on the basis of their electrophoretic mobility, as CYP4A3 (*upper band*) and CYP4A1 (*lower band*). Further identifications of CYP proteins were made as described in Fig. 2 and Table 1

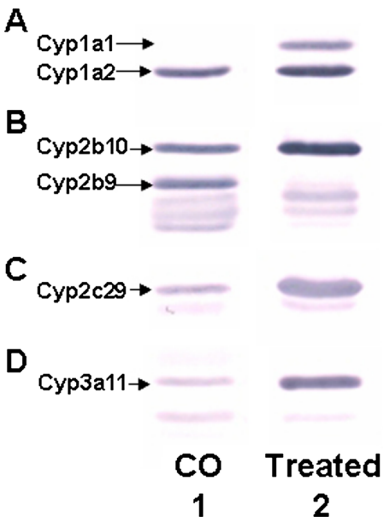


**Fig. 2** Immunoblots of microsomal CYP proteins isolated from livers of mice pretreated with CYP inducers. Pooled hepatic microsomes prepared from NF-, PB- and DEX-pretreated female wild-type C57BL/6 mice were used as positive controls to probe immunoblots containing induced CYP proteins to assess Cyp1a1/1a2, Cyp2b10 or Cyp2c29 and Cyp3a11 induction, respectively, and to aid in identifying CYP proteins. *Lane 1* contained hepatic microsomes from control (CO) untreated mice (5 μg protein). *Lane 2* contained microsomes from mice pretreated with NF (1 μg protein, *panel A*), PB (1 μg protein, *panel B*; 5 μg protein, *panel C*), or DEX (1 μg protein, *panel D*). Anti-CYP1A IgG detected one major band that corresponds to Cyp1a2 (*panel A*, *lower band*) because Cyp1a1 (*lane 1*, *panel A*, *upper band*) was undetectable in microsomes of control (CO) mice [42]. However, an upper band representing Cyp1a1 (*lane 2*, *panel A*) was detected in microsomes of mice pretreated with NF, a known Cyp1a1/1a2 inducer [43]. The lower Cyp1a2 band detected in microsomes was induced 10-fold by NF pretreatment of control mice. Anti-CYP2B IgG detected a major band in microsomes identified as Cyp2b10 (*panel B, upper band*) that was induced 15-fold (*lane 2*) by pretreatment of mice with PB, a potent Cyp2b10 inducer [54]. A second band identified as Cyp2b9 (*lane 1*) migrated just below Cyp2b10 and was not induced by PB (*lane 2*). Anti-mouse Cyp2c29 IgG (at a 1:1,000 dilution) detected one major band in microsomes identified as Cyp2c29 (*panel C, upper band*) that was induced 5-fold (*lane 2*) by pretreatment of mice with PB, a strong Cyp2c29 inducer [50]. Anti-CYP3A IgG detected a major band in microsomes (*panel D, upper band*) identified as Cyp3a11 that was induced 26-fold (*lane 2*) by pretreatment of mice with DEX, a potent Cyp3a11 inducer [52, 54]. Additional identifications of CYP proteins were made as described in Table 1

## Hepatic lithocholic acid hydroxylation

To assess the ability of hepatic microsomal CYP enzymes of *Bsep*$^{-/-}$ mice to metabolize and detoxify bile acids, we measured lithocholic acid hydroxylase activity in microsomes prepared from pooled livers of female and male *Bsep*$^{-/-}$ and wild-type (FVB/NJ × C57BL/6J) mice. Three major metabolites identified as murideoxycholic acid, 3-ketocholanoic acid and isolithocholic acid were detected (Table 3). Murideoxycholic acid is formed via hydroxylation of lithocholic acid at the 6β-position, 3-ketocholanoic acid formation proceeds via an initial 3β-hydroxylation followed by dehydration [38, 39] and isolithocholic acid formation involves a stereospecific reduction of 3-ketocholanoic acid mediated by unknown microsomal non-CYP enzymes [38]. In addition, a minor 6α-hydroxy metabolite identified as hyodeoxycholic acid and a second unidentified metabolite (*m/z* 389) were detected. No metabolites were detected in control incubations performed with boiled microsomes or without NADPH. Interestingly, small amounts of β-muricholic acid were detected when hepatic microsomes were incubated alone, indicating the presence of endogenous β-muricholic acid in the original microsomal samples.

## Effect of inhibitory CYP antibodies on lithocholic acid hydroxylation

To assess the contribution of mouse Cyp2b, Cyp2c and Cyp3a enzymes to lithocholic acid hydroxylation activities, varying amounts of anti-CYP2B, anti-CYP2C, or anti-CYP3A IgG were preincubated with hepatic microsomes isolated from male *Bsep*$^{-/-}$ (FVB/NJ × C57BL/6J) mice fed the normal or CA-enriched diet, and formation of 3-ketocholanoic acid and murideoxycholic acid metabolites was determined. The results indicate that anti-CYP3A IgG (at 5 mg IgG/mg protein) inhibited 3-ketocholanoic acid formation (lithocholic acid 3β-hydroxylase activity) by 48 and 56 % in hepatic microsomes of *Bsep*$^{-/-}$ mice fed the normal (Fig. 3a) or CA-enriched (Fig. 3b) diet, respectively, suggesting the involvement of Cyp3a enzymes. No inhibition was observed using anti-CYP2B, anti-CYP2C, or control IgG. Anti-CYP3A IgG (at 5 mg IgG/mg protein) inhibited murideoxycholic acid formation (lithocholic acid 6β-hydroxylase activity) by 47 % in hepatic microsomes from *Bsep*$^{-/-}$ mice fed the normal diet (data not shown). Again, no inhibition was observed using anti-CYP2B, anti-CYP2C, or control IgG. In contrast, anti-CYP2B, anti-CYP2C and anti-CYP3A IgG (at 5 mg IgG/mg protein) inhibited murideoxycholic acid formation by 32, 30 and 10 %, respectively, in hepatic microsomes from CA-fed *Bsep*$^{-/-}$ mice (data not shown). The results suggest that murideoxycholic acid formation in hepatic microsomes of male *Bsep*$^{-/-}$ mice fed the normal diet is catalyzed primarily by Cyp3a enzymes, whereas murideoxycholic acid formation in microsomes of CA-fed *Bsep*$^{-/-}$ mice is catalyzed by Cyp2b, Cyp2c and, to a lesser extent, Cyp3a enzymes, probably as a result of CA-elicited Cyp2b10 and Cyp2c29 induction. Moreover, hepatic microsomal Cyp2b10 and Cyp2c29 protein levels were increased 8.9- and 1.7-fold, respectively, by CA feeding of male *Bsep*$^{-/-}$ mice (Table 4). By comparison, Deo and Bandiera [38] reported that lithocholic acid 3β-hydroxylase activity was mediated primarily by CYP3A enzymes and

**Table 1** Hepatic microsomal CYP and mEH protein levels of wild-type and *Bsep*$^{-/-}$ mice

| Protein[a] | Identified enzyme[b] | Wild-type | | *Bsep*$^{-/-}$ | |
|---|---|---|---|---|---|
| | | Female ($n = 4$ or 6)[c] | Male ($n = 4$ or 6)[c] | Female ($n = 4$) | Male ($n = 4$) |
| Cyp2a(a) | Cyp2a5 | 1.00 ± 0.04 | 0.89 ± 0.06 | 0.77 ± 0.03 (0.8)[d] | 0.87 ± 0.03 (1.0) |
| Cyp2a(b) | Cyp2a4 | 1.00 ± 0.05 | n.d. | 1.05 ± 0.10 (1.1) | n.d. |
| Cyp2b(a) | Cyp2b10 | 1.00 ± 0.08 | 0.51 ± 0.12 | 0.94 ± 0.12 (0.9) | 0.37 ± 0.04 (0.7) |
| Cyp2b(b) | Cyp2b9 | 1.00 ± 0.03 | 0.16 ± 0.07 | 0.73 ± 0.11 (0.7) | n.d. |
| Cyp3a(a) | Cyp3a11 | 1.00 ± 0.07 | 1.80 ± 0.11 | 2.54 ± 0.16 (2.5)[d] | 3.70 ± 0.30 (2.1)[d] |
| Cyp3a(b) | Cyp3a41 | 1.00 ± 0.10 | n.d. | 0.61 ± 0.04 (0.6)[d] | n.d. |
| Cyp4a[e] | Unidentified | 1.00 ± 0.08 | 0.96 ± 0.14 | 0.51 ± 0.06 (0.5)[d] | 4.77 ± 0.13 (5.0)[d] |
| mEH | mEH | 1.00 ± 0.06 | 1.43 ± 0.10 | 2.75 ± 0.09 (2.8)[d] | 2.20 ± 0.11 (1.5)[d] |

Microsomes were prepared from individual livers of wild-type and *Bsep*$^{-/-}$ FVB/NJ mice fed the normal diet. CYP and mEH protein levels are expressed relative to levels of female wild-type mice set at 1.00. Values represent the mean ± SE for 4 or 6 mice per group, based on 2–7 experimental determinations. Numbers in parentheses denote levels of *bsep*$^{-/-}$ mice relative to those of wild-type mice of the same sex

[a] Mouse CYP proteins were assigned letter designations based on their relative electrophoretic mobility on polyacrylamide gels, so that CYP proteins with the lowest mobility (i.e. top band) were designated (a) and the CYP protein immediately below was designated (b)

[b] Mouse CYP proteins were identified on the basis of their relative electrophoretic mobility, reactivity with CYP antibodies and sex-dependent expression as described in the references below. Of the two hepatic Cyp2a enzymes, Cyp2a4 displays female-predominant expression and a lower expression level than Cyp2a5 [70]. Thus, the Cyp2a(a) protein band detected in female and male mice corresponds to Cyp2a5 and the Cyp2a(b) protein band that migrated immediately below Cyp2a5 and was detected only in female mice represents Cyp2a4. Of the Cyp2b proteins, Cyp2b10 has lower electrophoretic mobility and Cyp2b9 has slightly greater mobility and displays female-predominant expression [51, 54]. Thus, the bands designated as Cyp2b(a) and Cyp2b(b) correspond to Cyp2b10 and Cyp2b9, respectively. Of the Cyp3a proteins, Cyp3a11 has lower electrophoretic mobility [52–54, 71]. Cyp3a41 is expressed predominantly in female mice and displays slightly greater mobility than Cyp3a11 [54, 71]. Thus, the band designated as Cyp3a(a) corresponds to Cyp3a11 and the Cyp3a(b) band immediately below represents Cyp3a41

[c] Six wild-type female or male mice were used for Cyp2a, Cyp2b, and Cyp3a quantitation while four mice were used for Cyp4a and mEH quantitation

[d] Significantly different ($P < 0.05$) from the corresponding value of wild-type mice of the same sex

[e] One major unidentified Cyp4a protein was detected on immunoblots. See Fig. 1 for details

*n.d.*, non-detectable

lithocholic acid 6β-hydroxylase activity was catalyzed by CYP2C and CYP3A enzymes in rat hepatic microsomes.

## Effect of the CA-enriched diet on CYP and mEH expression

In a previous study, Wang et al. [17] reported that the mRNA expression of major mouse hepatic CYP (*Cyp2b10*, *Cyp3a11*, *Cyp3a16*) genes was increased in *Bsep*$^{-/-}$ mice by dietary CA administration. In the present study, we compared the relative protein expression of CYP, mEH and reductase enzymes in hepatic microsomes from *Bsep*$^{-/-}$ mice fed a CA-enriched diet or a normal diet. Densitometric quantitation of protein levels showed that hepatic microsomal Cyp2b10 protein levels were increased 4- to 9-fold and Cyp2c29, Cyp3a11 and mEH levels were increased 1.4- to 1.8-fold in female and male *Bsep*$^{-/-}$ mice fed a CA-enriched diet compared to *Bsep*$^{-/-}$ mice fed the normal diet (see Table 4). In contrast, Cyp1a2 and reductase levels (data not shown) were not affected appreciably. The modest increase in Cyp3a11 and mEH expression in *Bsep*$^{-/-}$ mice fed the CA-enriched diet was likely due to the already elevated Cyp3a11 and mEH protein levels observed in microsomes of *Bsep*$^{-/-}$ mice (see Table 1).

## Effect of Bsep inactivation on testosterone hydroxylation activities

To verify the physiological significance of alterations in CYP protein expression in *Bsep*$^{-/-}$ mice, we examined hepatic microsomal testosterone hydroxylation activities in *Bsep*$^{-/-}$ and wild-type mice. Total hepatic microsomal testosterone hydroxylation activities were approximately two-times greater in female and male *Bsep*$^{-/-}$ mice compared to wild-type mice (Table 5). Hepatic Cyp3a11-mediated testosterone 6β-hydroxylation [55], which forms the major testosterone metabolite in mice, was significantly increased (2.9- to 3.5-fold) in female and male *Bsep*$^{-/-}$ mice. Hepatic Cyp3a11-dependent testosterone 2β- and 15β-hydroxylation activities were significantly greater (2.1- to 2.2-times) in *Bsep*$^{-/-}$ mice. The observed increases in Cyp3a11-mediated testosterone 2β-, 6β- and 15β-hydroxylation activities were accompanied by similar increases in Cyp3a11 protein levels (see Table 1).

**Table 2** Relative hepatic *Cyp3a* mRNA levels of wild-type and *Bsep*$^{-/-}$ mice

| CYP gene | Wild-type | | *Bsep*$^{-/-}$ | |
|---|---|---|---|---|
| | Female ($n = 4$) | Male ($n = 4$) | Female ($n = 4$) | Male ($n = 4$) |
| *Cyp3a11* | 1.00 ± 0.22 | 1.95 ± 0.11 | 2.56 ± 0.33 (2.6)[a] | 3.79 ± 0.55 (2.0)[a] |
| *Cyp3a13* | 1.00 ± 0.13 | 1.26 ± 0.17 | 1.19 ± 0.13 (1.2) | 1.09 ± 0.13 (0.9) |
| *Cyp3a16* | 1.00 ± 0.17 | 1.76 ± 0.12 | 2.28 ± 0.16 (2.3)[a] | 3.68 ± 0.39 (2.1)[a] |
| *Cyp3a25* | 1.00 ± 0.07 | 1.23 ± 0.03 | 1.24 ± 0.11 (1.2) | 1.65 ± 0.18 (1.3) |
| *Cyp3a41* | 1.00 ± 0.18 | n.d. | 0.83 ± 0.38 (0.8) | n.d. |

Relative *Cyp3a* mRNA levels in individual livers of *Bsep*$^{-/-}$ and wild-type FVB/NJ mice fed the normal diet were quantified by RT-PCR and normalized against ribosomal protein S15 as outlined previously [17]. Levels are expressed relative to levels of female wild-type mice set at 1.00. Values are expressed as the mean ± SE for 4 mice per group. Numbers in parentheses denote levels of *Bsep*$^{-/-}$ mice relative to levels of wild-type mice of the same sex

*n.d.* non-detectable

[a] Significantly different ($P < 0.05$) from the corresponding value of wild-type mice of the same sex

**Table 3** Major metabolites of lithocholic acid in mouse hepatic microsomes

| Microsomal preparation | Metabolite (pmol formed/min/mg protein) | | |
|---|---|---|---|
| | MDCA | 3KCA[a] | ILCA[b] |
| Female wild-type | 1,392 ± 20 | 1,202 ± 31 | 142 ± 3 |
| Female *Bsep*$^{-/-}$ | 1,465 ± 19 | 1,064 ± 89 | 108 ± 5 |
| Male wild-type | 1,122 ± 23 | 1,400 ± 30 | 177 ± 11 |
| Male *Bsep*$^{-/-}$ | 1,740 ± 26 | 1,668 ± 59 | 155 ± 10 |

Lithocholic acid metabolism was determined in microsomes isolated from pooled livers of *Bsep*$^{-/-}$ and wild-type (FVB/NJ × C57BL/6J) mice fed the normal diet. Murideoxycholic acid (MDCA), 3-ketocholanoic acid (3KCA) and isolithocholic acid (ILCA) metabolites were identified by LC/MS. Values represent the mean ± SE from 3–4 experimental determinations

[a] 3KCA formation proceeds via an initial 3β-hydroxylation of lithocholic acid followed by dehydration [37]

[b] ILCA formation is proposed to involve a stereospecific reduction of 3KCA by unknown microsomal non-CYP enzymes [38]

## Effect of the CA-enriched diet on CYP-mediated enzyme activities

Total hepatic microsomal testosterone hydroxylation activity was increased 2-fold in CA-fed female and male *Bsep*$^{-/-}$ mice compared to *Bsep*$^{-/-}$ mice fed the normal diet (data not shown). Cyp3a11-mediated hepatic microsomal testosterone 2β-, 6β- and 15β-hydroxylation activities were increased 1.8- to 3.5-fold, while testosterone 15α-hydroxylase activity was increased 3.8- to 4-fold, in CA-fed female and male *Bsep*$^{-/-}$ mice (Fig. 4). The increase in testosterone hydroxylation activities in CA-fed *Bsep*$^{-/-}$ mice was likely due to enhanced levels of Cyp3a11 and other CYP enzymes (e.g. Cyp2b10, Cyp2c29) (see Table 4).

Mouse hepatic microsomal BROD, EROD and MROD activities have been used as biomarker activities for Cyp2b10 [56, 57], Cyp1a1 [57] and Cyp1a2 [57], respectively. A comparison of alkoxyresorufin *O*-dealkylation activities in hepatic microsomes of *Bsep*$^{-/-}$ mice fed the CA-enriched or normal diet is illustrated in Fig. 5. The results demonstrated a 6- to 12-fold increase in hepatic Cyp2b10-mediated BROD activity in CA-fed female and male *Bsep*$^{-/-}$ mice compared to *Bsep*$^{-/-}$ mice fed the normal diet. Hepatic EROD activity was increased 2.4- to 2.9-fold in CA-fed *Bsep*$^{-/-}$ mice, while MROD activity was increased slightly.

## Correlation of enzyme activities with CYP protein levels

The relationship between CYP protein levels and mouse hepatic microsomal BROD, EROD, testosterone hydroxylase and lithocholic acid hydroxylase activities was examined using hepatic microsomal samples prepared from female and male wild-type and *Bsep*$^{-/-}$ mice fed the CA-enriched or normal diet and coefficient of determination ($r^2$) values were obtained. The results (Table 6) show a strong correlation between hepatic microsomal BROD activity and Cyp2b10 protein levels, supporting a major role for Cyp2b10 in mediating this activity. EROD activity was well correlated to Cyp2c29 (Table 6) but not to Cyp1a2 (data not shown) protein levels. Because Cyp1a1 protein was undetectable in the mouse hepatic microsomal samples, the correlation results suggest that Cyp2c29 catalyzes hepatic microsomal EROD activity in non-induced mice. CYP2C enzymes are known to catalyze EROD activity in hepatic microsomes of untreated rats [47]. Strong correlations were observed for testosterone 2β-, 6β- and 15β-hydroxylation activities and Cyp3a11 protein levels, as was also demonstrated by Bornheim and Correia [55].

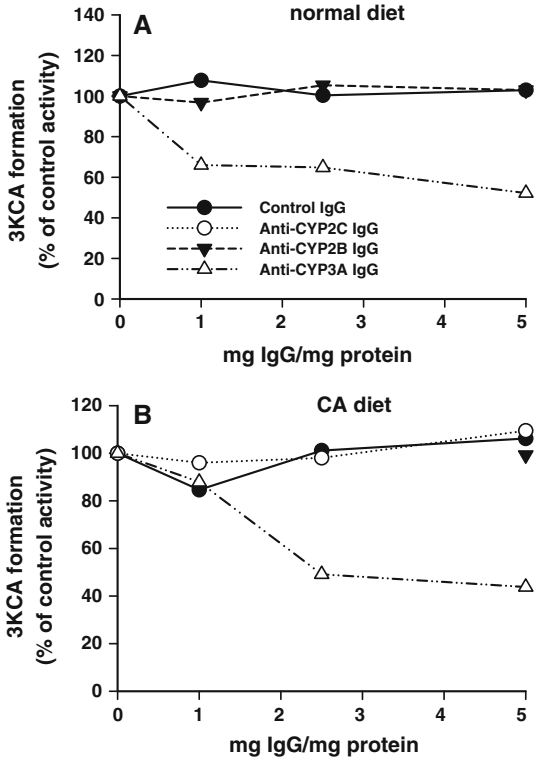


**Fig. 3** Effect of antibodies on hepatic microsomal lithocholic acid hydroxylation in male *Bsep*$^{-/-}$ mice. The effect of anti-rat CYP2B, anti-CYP2C, anti-CYP3A and control IgG on formation of 3-ketocholanoic acid (3KCA) (lithocholic acid 3β-hydroxylase activity) was determined using microsomes isolated from pooled livers of male *Bsep*$^{-/-}$ and wild-type (FVB/NJ × C57BL/6J) mice fed the normal (**a**) or CA-enriched (**b**) diet. Values represent the average of duplicate determinations and are expressed as % of control activity obtained in the absence of antibody. Microsomes were preincubated at 25 °C for 15 min with 1.0, 2.5 and 5.0 mg IgG/mg microsomal protein prior to addition of substrate, NADPH and subsequent assay. Antibodies are represented by *symbols* illustrated in **a**

Lithocholic acid 3β-hydroxylase activity (i.e. 3-ketocholanoic acid formation) was well correlated with Cyp3a11 protein levels, in agreement with the results of the antibody inhibition experiments (see Fig. 3a, b), which indicate a primary role for Cyp3a11 in lithocholic acid 3β-hydroxylation.

## Discussion

The *Bsep*$^{-/-}$ mouse is a unique model for investigating the biochemical consequences of intrahepatic cholestasis. In the present study, we demonstrated induction of hepatic Cyp3a11 mRNA and protein expression and associated enzyme activities in response to Bsep inactivation. Increased hepatic *Cyp3a/Cyp3a11* gene (or protein) expression was previously noted in *Pxr*$^{-/-}$ [40, 58–60], *Fxr*$^{-/-}$ [58, 61], *Cyp27a1*$^{-/-}$ [62] and *liver X receptor*$^{-/-}$ [63] mice. Taken together, the findings suggest that ablation of murine nuclear receptor genes involved in bile acid homeostasis results in the upregulation of *Cyp3a/Cyp3a11* expression, possibly as an adaptive hepatoprotective response to elevated hepatic bile acid levels. We propose that induction of hepatic Cyp3a11 is responsible for enhanced bile acid hydroxylation and increased production of novel tetrahydroxylated bile acids in *Bsep*$^{-/-}$ mice [8, 15]. Support for this hypothesis is provided by the correlation analysis, which indicated a positive correlation between hepatic microsomal lithocholic acid 3β-hydroxylase activity and Cyp3a11 protein levels, and by the antibody inhibition experiments showing that antibodies against CYP3A enzymes inhibit hepatic microsomal lithocholic acid 3β-hydroxylase activity in *Bsep*$^{-/-}$ mice.

Wang et al. [8, 15] had previously reported that *Bsep*$^{-/-}$ mice display a mild, nonprogressive, persistent form of intrahepatic cholestasis. Biliary secretion of hydrophobic bile salts such as cholate was greatly reduced in *Bsep*$^{-/-}$ mice (17-fold lower than in wild-type mice), while secretion of the more hydrophilic bile salts such as β-muricholate and ω-muricholate was maintained [8, 15]. In addition, concentrations of tetrahydroxylated bile acids were significantly greater in bile, liver and serum of *Bsep*$^{-/-}$ mice than wild-type mice [8, 19], indicating that *Bsep*$^{-/-}$ mice have an increased ability to hydroxylate and thereby detoxify hydrophobic bile acids. Elevated hydroxylation of bile salts in mice serves not only as a detoxification mechanism for hydrophobic bile salts, but can also facilitate clearance of the more hydrophilic bile salts from the

**Table 4** Effect of dietary CA administration on CYP and mEH protein levels in *Bsep*$^{-/-}$ mice

| Protein | Female *Bsep*$^{-/-}$ | | Male *Bsep*$^{-/-}$ | |
|---|---|---|---|---|
| | Normal diet | CA diet | Normal diet | CA diet |
| Cyp2b10 | 1.00 ± 0.17 | 3.53 ± 0.06 (3.5) | 0.36 ± 0.07 | 3.20 ± 0.23 (8.9) |
| Cyp2c29 | 1.00 ± 0.34 | 1.66 ± 0.17 (1.7) | 0.84 ± 0.11 | 1.42 ± 0.15 (1.7) |
| Cyp3a11 | 1.00 ± 0.08 | 1.72 ± 0.17 (1.7) | 1.28 ± 0.10 | 1.85 ± 0.11 (1.5) |
| mEH | 1.00 ± 0.05 | 1.82 ± 0.10 (1.8) | 1.29 ± 0.04 | 1.78 ± 0.05 (1.4) |

Microsomes were prepared from pooled livers of *Bsep*$^{-/-}$ (FVB/NJ × C57BL/6J) mice fed the normal or CA-enriched diet. Microsomal CYP and mEH protein levels represent the mean ± SE from 3–6 experimental determinations and are expressed relative to levels of female *Bsep*$^{-/-}$ mice set at 1.00. Numbers in parentheses denote CYP and mEH protein levels of CA-fed *Bsep*$^{-/-}$ mice relative to levels of *Bsep*$^{-/-}$ mice fed the normal diet

**Table 5** Hepatic testosterone hydroxylation activities of wild-type and *Bsep*$^{-/-}$ mice

| Metabolite | Wild-type (pmol formed/min/mg protein) | | *Bsep*$^{-/-}$ (pmol formed/min/mg protein) | |
|---|---|---|---|---|
| | Female ($n = 6$) | Male ($n = 6$) | Female ($n = 4$) | Male ($n = 4$) |
| 2α-OH | 43 ± 15 | 90 ± 30 | 110 ± 14 (2.6)[a] | 179 ± 14 (2.0) |
| 2β-OH | 427 ± 17 | 631 ± 256 | 924 ± 45 (2.2)[a] | 1,254 ± 39 (2.0) |
| 6α-OH | 575 ± 35 | 400 ± 47 | 324 ± 15 (0.6)[a] | 388 ± 46 (1.0) |
| 6β-OH | 3,840 ± 382 | 4,319 ± 560 | 11,217 ± 882 (2.9)[a] | 15,236 ± 598 (3.5)[a] |
| 7α-OH | 1,482 ± 67 | 1,144 ± 204 | 1,198 ± 68 (0.8)[a] | 1,416 ± 50 (1.2) |
| 15α-OH | 431 ± 32 | 356 ± 38 | 424 ± 19 (1.0) | 546 ± 19 (1.5)[a] |
| 15β-OH | 323 ± 23 | 250 ± 43 | 692 ± 34 (2.1)[a] | 863 ± 50 (3.5)[a] |
| 16α-OH | 341 ± 16 | 395 ± 39 | 383 ± 26 (1.1) | 278 ± 16 (0.7)[a] |
| 16β-OH | 281 ± 30 | 727 ± 75 | 567 ± 21 (2.0)[a] | 850 ± 42 (1.2) |
| Androstenedione | 1,435 ± 81 | 2,131 ± 148 | 1,417 ± 217 (1.0) | 2,431 ± 183 (1.1) |
| Total | 9,178 ± 579 | 10,442 ± 1,021 | 17,255 ± 1,265 (1.9)[a] | 23,440 ± 952 (2.2)[a] |

Testosterone hydroxylation activities were determined in microsomes isolated from individual livers of *Bsep*$^{-/-}$ and wild-type FVB/NJ mice fed the normal diet. Hydroxy metabolites are represented by an OH designation. Values represent the mean ± SE for 4 or 6 mice per group, based on duplicate experimental determinations. Numbers in parentheses denote activities of *Bsep*$^{-/-}$ mice relative to activities of wild-type mice of the same sex. The total specific CYP content of microsomes was 0.90 ± 0.05 (female wild-type), 1.01 ± 0.05 (male wild-type), 1.04 ± 0.07 (female *Bsep*$^{-/-}$) and 1.32 ± 0.09 (male *Bsep*$^{-/-}$) nmol/mg protein

[a] Significantly different ($P < 0.05$) from the corresponding value of wild-type mice of the same sex

hepatocyte via the alternative canalicular bile salt transport pathway involving Mdr1a/1b transport proteins [8, 12]. Although tetrahydroxylated bile salts have been detected in human fetal gallbladder bile and in samples obtained from cholestatic patients [64–67], it remains to be determined whether human canalicular MDR1 can serve as an alternative transporter for hydrophilic bile salts in humans.

Evidence from our studies and those of other investigators indicates similarities between human and mouse hepatic CYP3A-mediated metabolic pathways. For example, human hepatic lithocholic acid 3β-hydroxylase activity (3-ketocholanoic acid formation) and 6β-hydroxylase activity (murideoxycholic acid formation) were catalyzed by human CYP3A4 [37, 39, 40] and in the present study, we demonstrated that mouse hepatic lithocholic acid 3β-hydroxylase and 6β-hydroxylase activities were inhibited by CYP3A antibodies and that mouse lithocholic acid 3β-hydroxylase activity was correlated with hepatic Cyp3a11 protein levels. In addition, testosterone 6β-hydroxylase activity correlated with Cyp3a11 protein levels in mouse hepatic microsomes and is known to be catalyzed by CYP3A4 in human hepatic microsomes [36, 40].

Transport of bile acids across the hepatocyte involves three major events that include uptake of bile acids from portal blood across the sinusoidal plasma membrane, intrahepatocellular transport and secretion across the canalicular membrane into the bile canaliculus [33]. Hepatic mEH anchored in the sinusoidal plasma membrane of

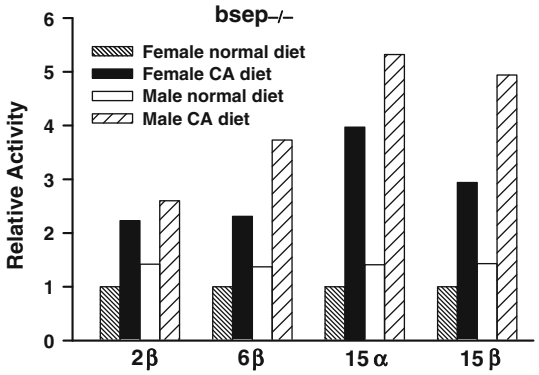


**Fig. 4** Effect of the CA-enriched diet on relative hepatic testosterone hydroxylation activities in *Bsep*$^{-/-}$ mice. Testosterone 2β-, 6β-, 15α- and 15β-hydroxylation activities were determined in microsomes prepared from pooled livers of *Bsep*$^{-/-}$ (FVB/NJ × C57BL/6J) mice fed the normal or CA-enriched diet. Activities represent the average or mean of 2–6 experimental determinations for each group and are expressed relative to activities of female *Bsep*$^{-/-}$ mice set at 1.00. The total specific CYP content of microsomes was 0.9 (female, normal diet), 1.7 (female, CA diet), 1.3 (male, normal diet) and 1.9 (male, CA diet) nmol/mg protein. *Error bars* are not shown because only 2 determinations were performed for some activities

humans and rodents can mediate uptake of bile acids from portal blood into the hepatocyte [24, 28]. In addition, an isoform of hepatic mEH embedded in the smooth endoplasmic reticular membrane of rats can translocate bile acids into the lumen of endoplasmic reticulum vesicles, which can then expel the bile acids from the sinusoidal into the canalicular compartment [32, 33]. Zhu et al. [28] found

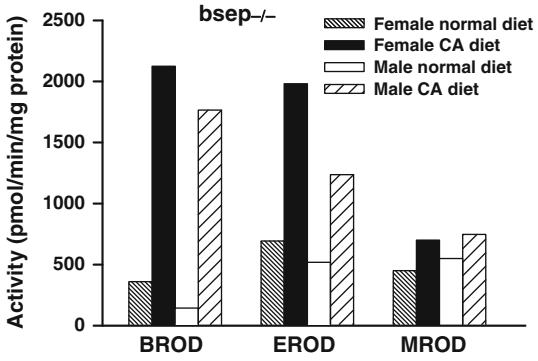


**Fig. 5** Effect of the CA-enriched diet on hepatic microsomal alkoxyresorufin *O*-dealkylation activities in *Bsep*$^{-/-}$ mice. BROD, EROD and MROD activities were determined in microsomes isolated from pooled livers of *Bsep*$^{-/-}$ (FVB/NJ × C57BL/6J) mice fed the normal or CA-enriched diet. Activities represent the average or mean of 2–4 experimental determinations for each group. *Error bars* are not shown because only 2 determinations were performed for some activities

**Table 6** Correlation of mouse hepatic enzyme activities and CYP protein levels

| Enzyme activity | CYP protein | Correlation ($r^2$) | *P* value |
|---|---|---|---|
| BROD | Cyp2b10 | 0.972 | <0.0001 |
| EROD | Cyp2c29 | 0.851 | 0.0011 |
| Testosterone 2β-hydroxylase | Cyp3a11 | 0.815 | 0.0021 |
| Testosterone 6β-hydroxylase | Cyp3a11 | 0.825 | 0.0018 |
| Testosterone 15β-hydroxylase | Cyp3a11 | 0.764 | 0.0045 |
| Lithocholic acid 3β-hydroxylase[a] | Cyp3a11 | 0.631 | 0.0186 |

Enzyme activity values and CYP protein level values from eight separate microsomal samples prepared from pooled livers of female and male *Bsep*$^{-/-}$ and wild-type (FVB/NJ × C57BL/6J) mice fed the normal or CA-enriched diet, respectively, were compared. Correlation analysis was performed to obtain the coefficient of determination ($r^2$). A *P* value of <0.05 was considered to be statistically significant

*BROD* benzyloxyresorufin *O*-debenzylase, *EROD* ethoxyresorufin *O*-deethylase

[a] Formation of the 3-ketocholanoic acid metabolite represents lithocholic acid 3β-hydroxylase activity [37]

that hepatic mEH mRNA and protein levels were very low in a patient who displayed elevated (~100-fold) serum bile salt levels (hypercholanemia) in the absence of hepatocellular injury, suggesting a defect in bile salt uptake across the sinusoidal hepatocyte plasma membrane. On the basis of this finding, Zhu and coworkers proposed that mEH plays a significant role in bile salt uptake in the human hepatocyte [28]. Moreover, Sinal et al. [10] reported increased hepatic mEH mRNA expression in *Fxr*$^{-/-}$ mice fed a CA-enriched diet. In the present study, we found that hepatic mEH protein levels were induced in *Bsep*$^{-/-}$ mice and that dietary CA administration further increased hepatic mEH protein expression.

Because *Bsep*$^{-/-}$ mice display a mild nonprogressive form of intrahepatic cholestasis and appear relatively normal [8], we suggest that these mice evolved adaptive defense mechanisms to reduce elevated hepatic bile acid concentrations and mitigate bile acid-elicited hepatoxicity. We propose that induced expression of Cyp3a11, Mdr1a/1b and mEH in *Bsep*$^{-/-}$ mice serves to reduce hepatic bile acid levels by three distinct pathways. First, bile acids entering the hepatocyte of *Bsep*$^{-/-}$ mice can be hydroxylated by Cyp3a11 in the endoplasmic reticular membrane. Because CYP-mediated bile acid hydroxylation generates more polar and less toxic hydroxy metabolites, Cyp3a11-mediated bile acid hydroxylation can provide an effective first level of defense for combating bile acid-elicited hepatotoxicity in mice. Second, a portion of the remaining bile acids can be effluxed from the hepatocyte into the bile canaliculus by an alternative canalicular bile salt transport pathway involving the Mdr1a/1b transporters [15], which are highly expressed in hepatic canalicular membranes of *Bsep*$^{-/-}$ mice [14, 15]. Third, bile acids remaining in the cytoplasm of the hepatocyte can be translocated by mEH, localized in the endoplasmic reticular membrane, into the lumen of endoplasmic reticulum vesicles, which can then expel the bile acids from the hepatocyte into bile by vesicular transport. This intrahepatocellular vesicular pathway for bile acid transport is recruited when an increased bile acid load is imposed upon the liver [33], which may be the case with *Bsep*$^{-/-}$ mice whose livers contain high concentrations of bile acids [8, 15]. However, the in vivo quantitative importance of the postulated mEH-vesicular bile acid transport pathway in mice and the relative contributions of the Cyp3a11, Mdr1a/1b and mEH-vesicular pathways to bile acid detoxification and efflux from hepatocytes of *Bsep*$^{-/-}$ mice remain to be determined.

In a previous study [17], it was shown that female and male *Bsep*$^{-/-}$ mice fed a CA-enriched diet developed more severe cholestatic symptoms. For example, the mRNA transcription profile in CA-challenged mice was consistent with cholestatic stress and impaired biliary secretion of bile acids as was evident by the overexpression of canalicular membrane transporters (Mdr1a/1b) and sinusoidal membrane bile acid efflux pumps (Mrp3, Mrp4) [17]. In the present study, hepatic Cyp3a11 and mEH protein levels were increased in female and male *Bsep*$^{-/-}$ mice by the CA-enriched diet, likely in response to elevated hepatic bile acid concentrations. Dietary CA administration also increased hepatic Cyp2b10 protein levels, BROD activity and Cyp2c29 protein expression in *Bsep*$^{-/-}$ mice. These results indicate that elevated hepatic CA levels regulate the expression of Cyp2b10, Cyp2c29, Cyp3a11 and mEH in *Bsep*$^{-/-}$ mice.

Murine hepatic *Cyp3a11* and *Cyp2b10* gene expression is regulated primarily by Pxr and the constitutive androstane receptor (Car), respectively, and both nuclear receptors function in a complementary manner with Fxr in the

regulation of bile acid metabolism and protection against bile acid-elicited hepatotoxicity [59, 61, 68]. Murine hepatic *Cyp1a*, *Cyp2a* and *Cyp2c* genes are also regulated by Pxr and Car [68]. Increased hepatic expression of *Cyp3a* and *Cyp2b* has been reported for CA-fed $Pxr^{-/-}$ [58, 69] and $Fxr^{-/-}$ [58, 61] mice. In addition, hepatic *Cyp3a11* and *Cyp2b10* gene expression was increased in $Pxr^{-/-}$ mice [40, 59, 60] and *Cyp3a11* gene expression was increased in $Car^{-/-}$ mice [60] that had been treated with lithocholic acid. These findings lead us to conclude that induction of hepatic *Cyp2b10*, *Cyp2c29* and *Cyp3a11* via transcriptional (or post-transcriptional) activation due to bile acid administration is a compensatory protective mechanism utilized by $Bsep^{-/-}$, $Car^{-/-}$, $Fxr^{-/-}$ and $Pxr^{-/-}$ mice to reduce elevated hepatic bile acid levels and bile acid-elicited hepatotoxicity. The mechanism presumably involves adaptive feedforward regulatory pathways for bile acid detoxification whereby the accumulating hepatic bile acids upregulate the expression of Cyp3a11, Cyp2b10 and Cyp2c29 enzymes, which in turn biotransform the hepatotoxic bile acids to less toxic hydroxy metabolites that can be conjugated and excreted.

In conclusion, the present study established that hepatic protein and mRNA levels of Cyp3a11 and associated enzyme activities, and hepatic protein levels of mEH, were increased in female and male mice as a consequence of Bsep inactivation and accompanying elevated hepatic bile acid levels. On the other hand, hepatic Cyp2b9 and Cyp3a41 protein levels were decreased in female mice as a result of Bsep inactivation, demonstrating the ability of Bsep to positively regulate Cyp2b9 and Cyp3a41 expression in female wild-type mice. Dietary CA administration increased expression of hepatic Cyp2b10, Cyp2c29, Cyp3a11 and mEH in $Bsep^{-/-}$ mice, indicating that CA is a key regulator of these enzymes in $Bsep^{-/-}$ mice. We propose that induced hepatic CYP enzymes, as well as the Mdr1a/1b canalicular bile salt transporters and possibly the mEH-vesicular bile acid transporter, serve, in the absence of Bsep, to reduce the buildup and toxicity of bile acids in the mouse hepatocyte.

**Acknowledgments** The authors are grateful to the Canadian Institutes of Health Research (Grant Number MOP-81174 to S. B. and Grant Number MOP-42560 to V. L.) for supporting this work. We also thank Drs. I. Kania-Korwel and H. J. Lehmler (University of Iowa) for supplying hepatic microsomes prepared from female wild-type mice. We appreciate the skilled assistance of Ms. Grace Leung in the preparation of several figures and the valued assistance of Mr. Chris Low in the treatment of mice.

## References

1. Hrycay EG, Bandiera SM (2008) Cytochrome P450 enzymes. In: Gad SC (ed) Preclinical development handbook: ADME and biopharmaceutical properties. Wiley, Hoboken, pp 627–696
2. Hrycay EG, Bandiera SM (2009) Expression, function and regulation of mouse cytochrome P450 enzymes: comparison with human cytochrome P450 enzymes. Curr Drug Metab 10:1151–1183 (Addendum in Curr Drug Metab 2010; 11:560)
3. Hrycay EG, Bandiera SM (2012) The monooxygenase, peroxidase, and peroxygenase properties of cytochrome P450. Arch Biochem Biophys 522:71–89
4. Hofmann AF (1999) The continuing importance of bile acids in liver and intestinal disease. Arch Intern Med 159:2647–2658
5. Hofmann AF (2002) Cholestatic liver disease: pathophysiology and therapeutic options. Liver 22(Suppl 2):14–19
6. Hofmann AF, Hagey LR (2008) Bile acids: chemistry, pathochemistry, biology, pathobiology, and therapeutics. Cell Mol Life Sci 65:2461–2483
7. Ling V, Wang R, Sheps JA (2011) Polyhydroxylated bile acids for treatment of biliary disorders. Patent Application Number: 20110263546
8. Wang R, Salem M, Yousef IM, Tuchweber B, Lam P, Childs SJ, Helgason CD, Ackerley C, Phillips MJ, Ling V (2001) Targeted inactivation of sister of P-glycoprotein gene (*spgp*) in mice results in nonprogressive but persistent intrahepatic cholestasis. Proc Natl Acad Sci USA 98:2011–2016
9. Kosters A, Karpen SJ (2008) Bile acid transporters in health and disease. Xenobiotica 38:1043–1071
10. Sinal CJ, Tohkin M, Miyata M, Ward JM, Lambert G, Gonzalez FJ (2000) Targeted disruption of the nuclear receptor FXR/BAR impairs bile acid and lipid homeostasis. Cell 102:731–744
11. Plass JRM, Mol O, Heegsma J, Geuken M, Faber KN, Jansen PLM, Müller M (2002) Farnesoid X receptor and bile salts are involved in transcriptional regulation of the gene encoding the human bile salt export pump. Hepatology 35:589–596
12. Zollner G, Fickert P, Fuchsbichler A, Silbert D, Wagner M, Arbeiter S, Gonzalez FJ, Marschall HU, Zatloukal K, Denk H, Trauner M (2003) Role of nuclear bile acid receptor, FXR, in adaptive ABC transporter regulation by cholic and ursodeoxycholic acid in mouse liver, kidney and intestine. J Hepatol 39:480–488
13. Childs S, Yeh RL, Hui D, Ling V (1998) Taxol resistance mediated by transfection of the liver-specific sister gene of P-glycoprotein. Cancer Res 58:4160–4167
14. Lam P, Wang R, Ling V (2005) Bile acid transport in sister of P-glycoprotein (ABCB11) knockout mice. Biochemistry 44:12598–12605
15. Wang R, Chen HL, Liu L, Sheps JA, Phillips MJ, Ling V (2009) Compensatory role of P-glycoproteins in knockout mice lacking the bile salt export pump. Hepatology 50:948–956
16. Strautnieks SS, Bull LN, Knisely AS, Kocoshis SA, Dahl N, Arnell H, Sokal E, Dahan K, Childs S, Ling V, Tanner MS, Kagalwalla AF, Németh A, Pawllowska J, Baker A, Mieli-Vergani G, Freimer NB, Gardiner RM, Thompson RJ (1998) A gene encoding a liver-specific ABC transporter is mutated in progressive familial intrahepatic cholestasis. Nat Genet 20:233–238
17. Wang R, Lam P, Liu L, Forrest D, Yousef IM, Mignault D, Phillips MJ, Ling V (2003) Severe cholestasis induced by cholic acid feeding in knockout mice of sister of P-glycoprotein. Hepatology 38:1489–1499
18. Davit-Spraul A, Gonzales E, Baussan C, Jacquemin E (2009) Progressive familial intrahepatic cholestasis. Orphanet J Rare Dis 4:1–12
19. Perwaiz S, Forrest D, Mignault D, Tuchweber B, Phillips MJ, Wang R, Ling V, Yousef IM (2003) Appearance of atypical 3α,6β7β12α-tetrahydroxy-5β-cholan-24-oic acid in spgp knockout mice. J Lipid Res 44:494–502
20. Megaraj V, Lida T, Jungsuwadee P, Hofmann AF, Vore M (2010) Hepatobiliary disposition of 3α,6α,7α,12α-tetrahydroxy-cholanoyl

taurine: a substrate for multiple canalicular transporters. Drug Metab Dispos 38:1723–1730
21. Miyata M, Kudo G, Lee YH, Yang TJ, Gelboin HV, Fernandez-Salguero P, Kimura P, Gonzalez FJ (1999) Targeted disruption of the microsomal epoxide hydrolase gene: microsomal epoxide hydrolase is required for the carcinogenic activity of 7,12-dimethylbenz[*a*]anthracene. J Biol Chem 274:23963–23968
22. Fretland AJ, Omiecinski CJ (2000) Epoxide hydrolases: biochemistry and molecular biology. Chem Biol Interact 129:41–59
23. Morisseau C, Newman JW, Wheelock CE, Hill T III, Morin D, Buckpitt AR, Hammock BD (2008) Development of metabolically stable inhibitors of mammalian microsomal epoxide hydrolase. Chem Res Toxicol 21:951–957
24. von Dippe P, Amoui M, Stellwagon RH, Levy D (1996) The functional expression of sodium-dependent bile acid transport in Madin-Darby canine kidney cells transfected with the cDNA for microsomal epoxide hydrolase. J Biol Chem 271:18176–18180
25. Ananthanarayanan M, Bucuvalas JC, Shneider BL, Sipple CJ, Suchy FJ (1991) An ontogenically regulated 48-kDa protein is a component of the $Na^+$-bile acid cotransporter of rat liver. Am J Physiol-Gastrointest Liver Physiol 261:G810–G817
26. von Dippe P, Amoui M, Alves C, Levy D (1993) $Na^+$-dependent bile acid transport by hepatocytes is mediated by a protein similar to microsomal epoxide hydrolase. Am J Physiol- Gastrointest Liver Physiol 264:G528–G534
27. Zhu QS, von Dippe P, Xing W, Levy D (1999) Membrane topology and cell surface targeting of microsomal epoxide hydrolase: evidence for multiple topological orientations. J Biol Chem 274:27898–27904
28. Zhu QS, Xing W, Qian B, von Dippe P, Shneider BJ, Fox VL, Levy D (2003) Inhibition of human m-epoxide hydrolase gene expression in a case of hypercholanemia. Biochim Biophys Acta 1638:208–216
29. Kullak-Ublick GA, Stieger B, Hagenbuch B, Meier PJ (2000) Hepatic transport of bile salts. Sem Liver Dis 20:273–292
30. Stieger B (2011) The role of the sodium-taurocholate cotransporting polypeptide (NTCP) and of the bile salt export pump (BSEP) in physiology and pathophysiology of bile formation. Handb Exp Pharmacol 201:205–259
31. von Dippe P, Zhu QS, Levy D (2003) Cell surface expression and bile acid transport function of one topological form of m-epoxide hydrolase. Biochem Biophys Res Commun 309:804–809
32. Alves C, von Dippe P, Amoui M, Levy D (1993) Bile acid transport into hepatocyte smooth endoplasmic reticulum vesicles is mediated by microsomal epoxide hydrolase, a membrane protein exhibiting two distinct topological orientations. J Biol Chem 268:20148–20155
33. Arrese M, Pizarro M, Solís N, Accatino L (1997) Adaptive regulation of hepatic bile salt transport: role of bile salt hydrophobicity and microtubule-dependent vesicular pathway. J Hepatol 26:694–702
34. Crawford JM, Berken CA, Gollan JL (1988) Role of the hepatocyte microtubular system in the excretion of bile salts and biliary lipid: implications for intracellular vesicular transport. J Lipid Res 29:144–156
35. Erlinger S (1996) Do intracellular organelles have any role in transport of bile acids by hepatocytes? J Hepatol 24(Suppl 1):88–93
36. Araya Z, Wikvall K (1999) 6α-Hydroxylation of taurochenodeoxycholic acid and lithocholic acid by CYP3A4 in human liver microsomes. Biochim Biophys Acta 1438:47–54
37. Bodin K, Lindbom U, Diczfalusy U (2005) Novel pathways of bile acid metabolism involving CYP3A4. Biochim Biophys Acta 1687:84–93
38. Deo AK, Bandiera SM (2008) Biotransformation of lithocholic acid by rat hepatic microsomes: metabolite analysis by liquid chromatography/mass spectrometry. Drug Metab Dispos 36:442–451
39. Deo AK, Bandiera SM (2009) 3-Ketocholanoic acid is the major in vitro human hepatic microsomal metabolite of lithocholic acid. Drug Metab Dispos 37:1938–1947
40. Xie W, Radominska-Pandya A, Shi Y, Simon CM, Nelson MC, Ong ES, Waxman DJ, Evans RM (2001) An essential role for nuclear receptors SXR/PXR in detoxification of cholestatic bile acids. Proc Natl Acad Sci USA 98:3375–3380
41. Deo AK, Bandiera SM (2008) Identification of human hepatic cytochrome P450 enzymes involved in the biotransformation of cholic and chenodeoxycholic acid. Drug Metab Dispos 36:1983–1991
42. Wong A, Bandiera SM (1996) Inductive effect of Telazol® on hepatic expression of cytochrome P450 2B in rats. Biochem Pharmacol 52:735–742
43. Kania-Korwel I, Hrycay EG, Bandiera SM, Lehmler HJ (2008) 2,2′3,3′6,6′-Hexachlorobiphenyl (PCB 136) atropisomers interact enantioselectively with hepatic microsomal cytochrome P450 enzymes. Chem Res Toxicol 21:1295–1303
44. Omura T, Sato R (1964) The carbon monoxide-binding pigment of liver microsomes. I. Evidence for its hemoprotein nature. J Biol Chem 239:2370–2378
45. Lowry OH, Rosebrough NJ, Farr AL, Randall RJ (1951) Protein measurement with the Folin phenol reagent. J Biol Chem 193:265–275
46. Anderson MD, Bandiera SM, Chang TKH, Bellward GD (1998) Effect of androgen administration during puberty on hepatic CYP2C11, CYP3A, and CYP2A1 expression in adult female rats. Drug Metab Dispos 26:1031–1038
47. Burke MD, Thompson S, Weaver RJ, Wolf CR, Mayer RT (1994) Cytochrome P450 specificities of alkoxyresorufin *O*-dealkylation in human and rat liver. Biochem Pharmacol 48:923–936
48. Hrycay EG, Bandiera SM (2003) Spectral interactions of tetrachlorobiphenyls with hepatic microsomal cytochrome P450 enzymes. Chem Biol Interact 146:285–296
49. Ryan DE, Thomas PE, Levin W (1980) Hepatic microsomal cytochrome P-450 from rats treated with isosafrole. J Biol Chem 255:7941–7955
50. Meyer RP, Hagemeyer CE, Knoth R, Kurz G, Volk B (2001) Oxidative hydrolysis of scoparone by cytochrome P450 CYP2C29 reveals a novel metabolite. Biochem Biophys Res Commun 285:32–39
51. Jarukamjorn K, Sakuma T, Miyaura JI, Nemoto N (1999) Different regulation of the expression of mouse hepatic cytochrome P450 2B enzymes by glucocorticoid. Arch Biochem Biophys 369:89–99
52. Schuetz EG, Schmid W, Schutz G, Brimer C, Yasuda K, Kamataki T, Bornheim L, Myles K, Cole TJ (2000) The glucocorticoid receptor is essential for induction of cytochrome P-4502B by steroids but not for drug or steroid induction of Cyp3A or P-450 reductase in mouse liver. Drug Metab Dispos 28:268–278
53. Schuetz EG, Umbenhauer DR, Yasuda K, Brimer C, Nguyen L, Relling MV, Schuetz JD, Schinkel AH (2000) Altered expression of hepatic cytochromes P-450 in mice deficient in one or more *mdr1* genes. Mol Pharmacol 57:188–197
54. Yamada H, Gohyama N, Honda SI, Hara T, Harada N, Oguri K (2002) Estrogen-dependent regulation of the expression of hepatic Cyp2b and 3a isoforms: assessment using aromatase-deficient mice. Toxicol Appl Pharmacol 180:1–10
55. Bornheim LM, Correia MA (1990) Selective inactivation of mouse liver cytochrome P-450IIIA by cannabidiol. Mol Pharmacol 38:319–326
56. Bornheim LM, Correia MA (1989) Purification and characterization of a mouse liver cytochrome P-450 induced by cannabidiol. Mol Pharmacol 36:377–383

57. Nerurkar PV, Park SS, Thomas PE, Nims RW, Lubet RA (1993) Methoxyresorufin and benzyloxyresorufin: substrates preferentially metabolized by cytochromes P4501A2 and 2B, respectively, in the rat and mouse. Biochem Pharmacol 46:933–943
58. Guo GL, Lambert G, Negishi M, Ward JM, Brewer HB Jr, Kliewer SA, Gonzalez FJ, Sinal CJ (2003) Complementary roles of farnesoid X receptor, pregnane X receptor, and constitutive androstane receptor in protection against bile acid toxicity. J Biol Chem 278:45062–45071
59. Staudinger JL, Goodwin B, Jones SA, Hawkins-Brown D, MacKenzie KI, LaTour A, Liu Y, Klaassen CD, Brown KK, Reinhard J, Willson TM, Koller BH, Kliewer SA (2001) The nuclear receptor PXR is a lithocholic acid sensor that protects against liver toxicity. Proc Natl Acad Sci USA 98:3369–3374
60. Zhang J, Huang W, Qatanani M, Evans RM, Moore DD (2004) The constitutive androstane receptor and pregnane X receptor function coordinately to prevent bile acid-induced hepatotoxicity. J Biol Chem 279:49517–49522
61. Schuetz EG, Strom S, Yasuda K, Lecureur V, Assem M, Brimer C, Lamba J, Kim RB, Ramachandran V, Komoroski BJ, Venkataramanan R, Cai H, Sinal CJ, Gonzalez FJ, Schuetz JD (2001) Disrupted bile acid homeostasis reveals an unexpected interaction among nuclear hormone receptors, transporters, and cytochrome P450. J Biol Chem 276:39411–39418
62. Goodwin B, Gauthier KC, Umetani M, Watson MA, Lochansky MI, Collins JL, Leitersdorf E, Mangelsdorf DJ, Kliewer SA, Repa JJ (2003) Identification of bile acid precursors as endogenous ligands for the nuclear xenobiotic pregnane X receptor. Proc Natl Acad Sci USA 100:223–228
63. Gnerre C, Schuster GU, Roth A, Handschin C, Johansson L, Looser R, Parini P, Podvinec M, Robertsson K, Gustafsson JJ, Meyer UA (2005) LXR deficiency and cholesterol feeding affect the expression and phenobarbital-mediated induction of cytochromes P450 in mouse liver. J Lipid Res 46:1633–1642
64. Setchell KD, Dumaswala R, Colombo C, Ronchi M (1988) Hepatic bile acid metabolism during early development revealed from the analysis of human fetal gallbladder bile. J Biol Chem 263:16637–16644
65. Bremmelgaard A, Sjovall J (1980) Hydroxylation of cholic, chenodeoxycholic, and deoxycholic acids in patients with intrahepatic cholestasis. J Lipid Res 21:1072–1081
66. Nakagawa M, Setchell KD (1990) Bile acid metabolism in early life: studies of amniotic fluid. J Lipid Res 31:1089–1098
67. Yousef IM, Bouchard G, Tuchweber B, Plaa GL (1997) Monohydroxy bile acid induced cholestasis: role of biotransformation. Drug Metab Rev 29:167–181
68. Wang H, Negishi M (2003) Transcriptional regulation of cytochrome P450 2B genes by nuclear receptors. Curr Drug Metab 4:515–525
69. Teng S, Piquette-Miller M (2007) Hepatoprotective role of PXR activation and MRP3 in cholic acid-induced cholestasis. Br J Pharmacol 151:367–376
70. Harada N, Negishi M (1984) Mouse liver testosterone 15α-hydroxylase (cytochrome P-45015α). Purification, regioselectivity, stereospecificity, and sex-dependent expression. J Biol Chem 259:1265–1271
71. Sakuma T, Takai M, Endo Y, Kuroiwa M, Ôhara A, Jarukamjorn K, Honma R, Nemoto N (2000) A novel female-specific member of the CYP3A gene subfamily in the mouse liver. Arch Biochem Biophys 377:153–162